Colloid Polym Sci 273:242–251 (1995)

ORIGINAL CONTRIBUTION

R. Makhloufi
J.-L. Mansot
E. Hirsch
J. Wéry
S.-J. Candau
D. Thomas
J.-P. Rolland

Electron microscopy and light scattering study of organometallic inverse micellar systems

Received: 18 May 1994
Accepted: 17 August 1994

R. Makhloufi (✉)
Laboratoire de Physique des Liquides et des Interfaces Groupe polymères
Université de Metz
1 Bd. Arago
57070 Metz, France

J.L. Mansot · J. Wéry
Laboratoire de Physique Cristalline
Institut des Matériaux de Nantes
UMR 110-Universités de Nantes
2 rue de la Houssiniére
44072 Nantes Cédex 03, France

E. Hirsch · S.-J. Candau
Laboratoire de spectrometrie et d'imagerie ultrasonores
Université Louis Pasteur
URA 851
4 rue Blaise Pascal
67070 Strasbourg Cédex, France

D. Thomas · J.-P. Rolland
Laboratoire de Biologie Cellulaire
URA 256
Université de Rennes I
Avenue du Général Leclerc
35042 Rennes, France

Abstract Colloidal dispersions in hydrocarbons of lead and calcium salts of isooctanoic acids are studied by means of Transmission Electron Microscopy and Light Scattering. The complementary results obtained, using each technique, allow us to investigate the structure of the mineral core, the size and the morphology of the colloidal particles. Special attention is paid to the aggregation properties of the metal salts particles as a function of the dilution and solvent.

Key words Colloidal dispersions – organometallic micellar systems – microscopic structure – microscopic properties

Introduction

Organometallic reverse micellar systems are of great interest for industrial applications because such systems permit the formation of stable dispersions of small mineral particles ($1 < \text{size} < 50$ nm) in hydrocarbons [1]. Depending on the nature and the structure of the mineral core of the micelles, these systems may have catalytic, anticorrosive or magnetic properties, among others [1–3]. These systems have wide applications in various industries (painting, lubrication, etc.). It is, however, known empirically that the properties of the dispersions and, more specifically, their stability are very sensitive to the method of synthesis and the chemical nature of the organic salts. It is therefore important to study the possible correlation between the microscopic structure of the dispersed particles and the macroscopic properties of the dispersion. The heterogeneous nature of the particles composed of a mineral core surrounded by an organic layer requires for structural

investigation the use of two complementary techniques. Ottewill et al. used small-angle neutron scattering and light scattering to investigate dispersions of calcium carbonate in toluene, stabilized by an alkylaryl sulphonic acid [4, 5].

In this paper we report a study by Quasi-Elastic Light Scattering (QELS) and Transmission Electron Microscopy (TEM) of metallic salts of isooctanoic acid in hydrocarbons, the metallic ions being lead and calcium. These systems are used industrially as siccative additives for paints. Special attention has been paid to so-called over based systems where the dispersions are made up of non-stoichiometric salts. In this case the metallic cations are introduced in excess in the solutions either as oxide or carbonate cations.

Materials

The systems studied consist of metallic salts of isooctanoic acids dispersed in hydrocarbons. Isooctanoic acids are mixtures of branched C8 acids containing dimethylhexanoic acid as major components with branching predominantly in the non-alpha position of the carboxylic group. Isooctanoic acids are available as Cekanoic C8 acids from Exxon Chemical.

Two types of salts were studied:

- a salt with a stoichiometric content of lead
- two non-stoichiometric calcium salt containing an excess of calcium.

The synthesis of such compounds, in non-aqueous media, is well described elsewhere [6, 7].

In the case of the Pb salt the chemical reaction is followed:

$$PbO + 2\ R\text{–}COOH \xrightarrow[\text{heated up to } 120\,^{\circ}C]{\text{White spirit}} H_2O + (RCOO)_2Pb$$

$$R = CH_3\text{–}CH(CH_3)\text{–}CH_2\text{–}CH(CH_3)\text{–}CH_2\text{–}$$

In the case of calcium salts the reaction is polyphasic (liquid/solid/gas) and more complex. It can be schematically described as follows for the over based salt with 60% of Ca in excess.

$$2\,Ca(OH)_2 + 2\,RCOOH + CO_2 \xrightarrow[\text{MeOH, } NH_4OH,\ \text{heating}]{\text{White spirit, Phase transfer}} H_2O + (RCOO)_2Ca,\ CaCO_3$$

At the end of the synthesis the reactional media were filtered and the remaining water was stripped by heating to 120 °C.

The remaining clear liquids were directly used after dilution for Transmission Electron Microscopy and Light Scattering experiments.

Experimental techniques

Transmission electron microscopy

The experiments were performed on an analytical Philips CM 30 electron microscope operating at 200 kV with an LaB_6 cathode. Both imaging and electron diffraction technique were used to obtain geometrical (size and shape) and structural (crystallinity) information [8]. All the examinations have been carried out in low electron dose conditions in order to avoid irradiation damage in the samples [9].

Sample preparation for the conventional TEM study

The two types of salts are characterized by the scattering power of their mineral core. In the case of calcium salts, the direct TEM examination of the micelles is difficult, due to the flow elastic scattering cross-section of carbon and calcium atoms. Consequently, methods including platinum shadowing are best preferred. For lead salts, the high elastic scattering cross-section of lead atoms allows us to visualize the mineral part of the micelles by direct examination in conventional TEM. In order to obtain reliable information on the size of the micelles two types of techniques are used: Cryopreparation techniques in order to study the micelles in their original medium and direct deposition methods which allow us to characterize the stability of the micelles and their ability to aggregate.

Calcium salts preparation methods for TEM examinations

The freeze-fracturing technique [10, 11] is used to study the over based calcium micelles in their original medium (Fig. 1a). A small droplet (0.5 mm diameter) of a diluted micellar dispersion in dodecane is rapidly quenched by immersion into melting nitrogen (T = 63 K). The frozen sample is then introduced under vacuum (10^{-7} mm Hg) and maintained at a temperature of 150K in order to avoid the recrystallization of the solvent.

The droplet is then fractured under vacuum, in order to create clean fracture surfaces, and a shadowed platinum/carbon replica (shadowing angle 45°) is carried out in order to reveal the morphology of the colloidal particles (the fracture propagates at the interface particle/solvent).

Colloid & Polymer Science, Vol. 273, No. 3 (1995)

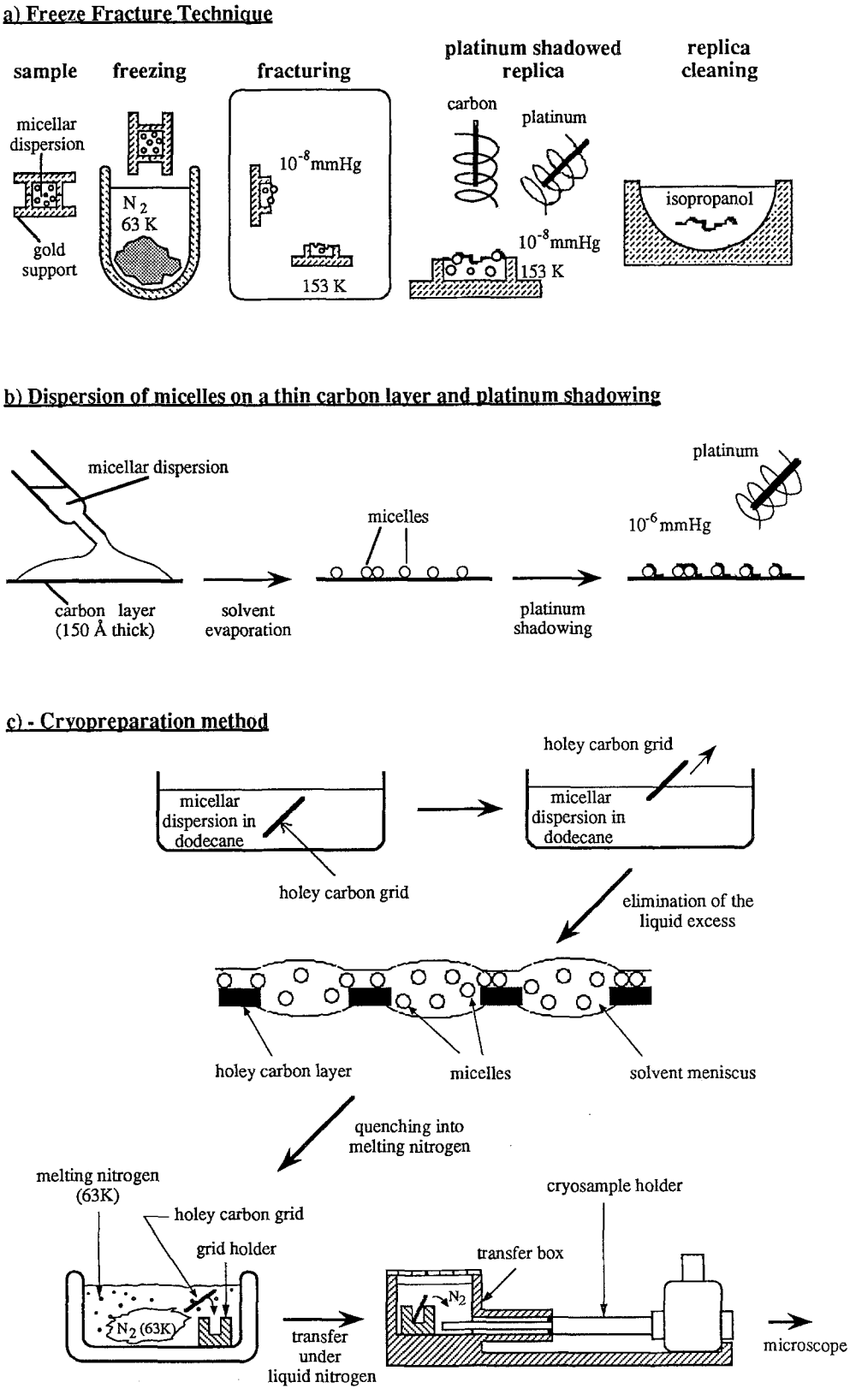

Fig. 1 Schematic representation of sample: a) Freeze fracturing technique b) Direct deposit and platinum shadowing c) Cryofixation

The sample is then warmed up to room temperature under atmospheric pressure. The replica is washed into isopropanol and deposited onto a copper grid for TEM examination.

For the direct deposit method (Fig. 1b) [11], a droplet of a highly diluted dispersion into hexane is deposited onto a carbon grid. After evaporation of the solvent the sample is introduced under vacuum and a platinum shadowing (shadowing angle 45°) is carried out in order to visualize the shape of the particles, out of their original medium. On this type of specimen, non shadowed parts allow us to carry out diffraction experiments on the micelles or aggregates.

Lead salts preparation methods for TEM examinations

As previously mentioned for lead salts, the direct examination of the mineral part of the micelles is preferred.

In order to study the micelles in their original medium, a cryopreparation method is used (Fig. 1c). A porous carbon grid is dipped into a diluted dispersion of lead isooctanoate in dodecane. After removing the excess liquid, the sample is quenched by immersion into melting nitrogen (63 K) and transferred under liquid nitrogen in the cryosample holder. The thus vitrified sample is then introduced in the microscope and maintained at a temperature of 120 K. During the examination the contamination is reduced by means of an anticontamination system surrounding the specimen and cooled at 77 K.

For the study of the lead salt, out of its liquid medium, one drop of a highly diluted dispersion of the salt in hexane is deposited onto a carbon film. After evaporation of the solvent the particles stick onto the carbon layer and the mineral part can be directly visualized in TEM.

Quasi-elastic scattering

Quasi-elastic light scattering experiments were performed at 25 °C on diluted solutions on the same apparatus as described elsewhere [12]. The volume fraction of the dispersed phase was varied from ϕ to $\phi/10$ where ϕ is the concentration of the original preparation.

The measurements involved the autocorrelation function of the intensity of the light scattered by the micellar solutions. This function was analyzed by means of the cumulant methods [13] in order to yield the variance v of the function and the first reduced cumulant $\langle\Gamma\rangle/2K^2$, where $\langle\Gamma\rangle$ is the average decay rate of the autocorrelation function and the magnitude of the scattering wave vector given by:

$$K = [4\pi n \sin(\theta/2)]/\lambda$$

θ is the scattering angle and λ the wavelength of the incident light in vacuo.

In the case of solutions of monodisperse particles, $\langle\Gamma\rangle/2K^2$ is equal to the translational diffusion coefficient of the particles. In the case of polydisperse aggregates however, $\langle\Gamma\rangle/2K^2$ is a mean diffusion coefficient given by [14]:

$$\langle\Gamma\rangle/2K^2 = \sum_i N_i M_i^2 D_i \Big/ \sum_i N_i M_i^2 ,$$

where N_i is the number of particles of mass M_i having a diffusion coefficient D_i. The variance v characterizes in this case the width of the distribution associated with $\langle\Gamma\rangle/2K^2$ and is given by:

$$V = (\langle D^2\rangle - (\langle D\rangle)^2/(\langle D\rangle)^2 .$$

More specifically, in the case of a distribution of hard spheres or radius R, the variance is:

$$V = \frac{\langle R^6\rangle\langle R^4\rangle}{(\langle R^5\rangle)^2} - 1 ,$$

where $\langle R^\gamma\rangle$ is given by:

$$\langle R^\gamma\rangle = \sum_i N_i R_i^\gamma \Big/ \sum_i N_i .$$

Moreover, for a dilute suspension of spherical particles, the variations of $\langle\Gamma\rangle/2K^2$ with the volume fraction ϕ of the dispersed phase is described by [15]:

$$\langle\Gamma\rangle/2K^2 = \frac{k_B T}{6\pi\eta R_H}(1 + k_D\phi) , \qquad (1)$$

where k_B is Boltzmann's constant, T the absolute temperature of the solution, η the viscosity of the solvent, R_H the mean hydrodynamic radius of the particles (equal to the radius R in the case of hard spheres) and k_D an hydrodynamic interaction parameter. For hard spheres systems, $k_D = 1.5$.

For more concentrated solutions, deviations to relation (1) may be observed, as a result of the interactions. More specifically, if the dispersed particles exhibit a size distribution, it has been shown by Pusey et al. [16] that the autocorrelation function is the sum of two distributions of exponentials, the ratio of the two average time constants increasing with the particle volume fraction (or concentration). The slowest of the two modes in associated with self-diffusion of particles and this effect leads to a decrease of the apparent diffusion coefficient $\langle\Gamma\rangle/2K^2$ as determined by a cumulant method, when the concentration is increased.

Sample preparation

The original samples were diluted, without any further purifications, with either a standard solvent (white spirit)

Colloid & Polymer Science, Vol. 273, No. 3 (1995)

or very pure grade heptane. The samples were then carefully filtered an centrifugated directly in the measuring cells for at least 2 h at 8000 g, before use.

Results

Electron microscopy

Lead salt study

Figure 2 presents a dark field image, obtained with a 50 μm objective aperture, and the corresponding selected area (1 μm diameter) electron diffraction pattern obtained on the frozen lead stoichiometric salt specimen.

The diffraction pattern presents mainly one enlarged Debye–Scherrer ring which points out the existence of short-range order. A high scattering background due to the solvent does not allow us to see if others rings are present.

The dark field image reveals the mineral core of the lead isooctanoate micelles as a small bright area with size of 10 to 15 Å. The homogeneous distribution of the particles in the sample demonstrates the well-vitrified state of the sample (no segregation artefacts). The total size of the micelles can be deduced by addition of twice the length of the isooctanoic radical to the size of the mineral core. This leads to a total diameter of about 30–35 Å.

In the case of the direct deposit method, the bright field and dark filed images and the diffraction pattern are presented in Fig. 3.

On the bright image two types of particles are clearly visible. The smaller ones are in the size range 10 to 15 Å as in the frozen sample and could correspond to the mineral core of single micelles. The diameter of the other population encountered in the highly concentrated region of the sample is in the range 30–60 Å and is interpreted as the aggregation of some micelles. This is confirmed by the examination of the corresponding dark field image (Fig. 2b) where the organized mineral cores appear as bright spots. Such an aggregation occurs during the hexane evaporation in the sample preparation process. These electron micrographs and the corresponding diffraction pattern which exhibits two enlarged Debye–Scherrer rings point out the ability of these micelles to form large organized particles when their environment is changed.

Calcium salts study

Figure 4 presents an electron micrograph obtained on a platinum shadowed replica prepared by the cryofracture technique on a dispersion of a calcium salt (60% excess of Ca) into dodecane. The picture clearly reveals the presence of spherical particles (micelles) well dispersed in the solvent, pointing out the absence of segregation artefacts. The diameter of the micelles deduced from the electron micrograph lies in the range 100 ± 15 Å.

The bright field image presented in Fig. 5 was obtained on platinum shadowed samples of overbased calcium salts with a calcium excess 60% prepared by the direct deposit method. Many spherical particles are clearly visible whose diameter lies in the range 100 ± 15 Å, respectively. The considerable absolute error of these measurements is due

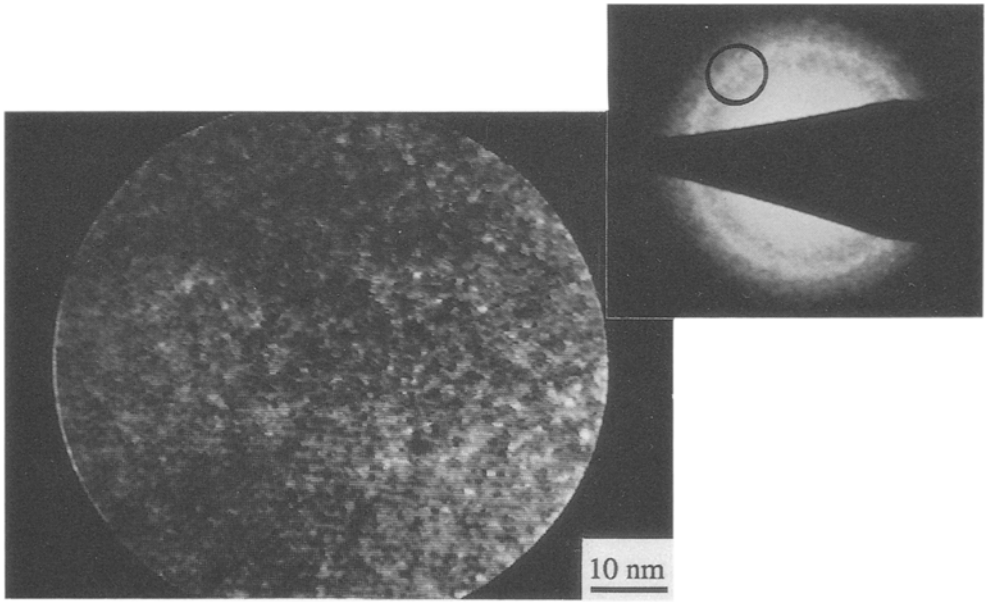

Fig. 2 Lead stoichiometric salt micrographs obtained on the cryofixed sample. a) Selected area electron diffraction carried out on a 1 μm diameter zone. It exhibits a strong diffusion background at low angle, due to the solvent, and a rather well defined Debye–Scherrer ring pointing out the existence of short range order in the mineral core of the micelles. b) Dark field image obtained with a 50 μm diameter ($\Omega = 11$ mrad) objective aperture (black circle on (a)). The highly scattering mineral cores of the micelles appear as small bright areas whose size is in the range 10 to 15 Å

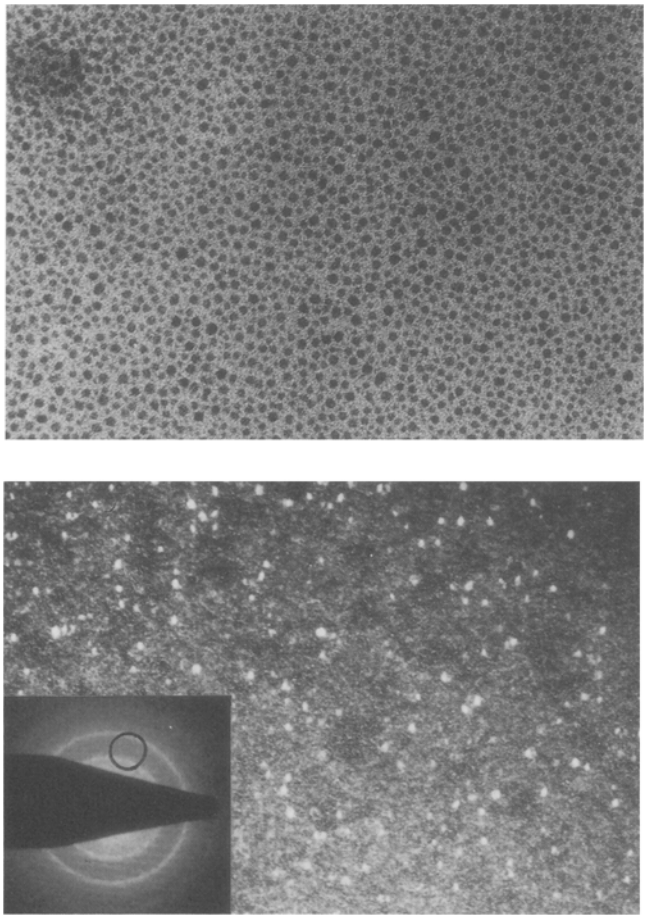

Fig. 3 Electron micrographs obtained on lead stoichiometric salt prepared by the direct deposit method: a) Bright field image showing mineral part of aggregates. In the low concentrated zone, the sizes of the particles (10 to 20 Å) are in agreement with those found by the cryopreparation method. In the high concentrated zone, the larger particles (50 – 70 Å) could be due to the aggregation of some micelles during the evaporation of the solvent. b) Dark field image and corresponding selected area electron diffraction pattern. The diffraction pattern exhibits two broad Debye–Scherrer rings pointing out the organized nature of the mineral core of the aggregates. These last ones appear as bright areas in the dark field micrograph

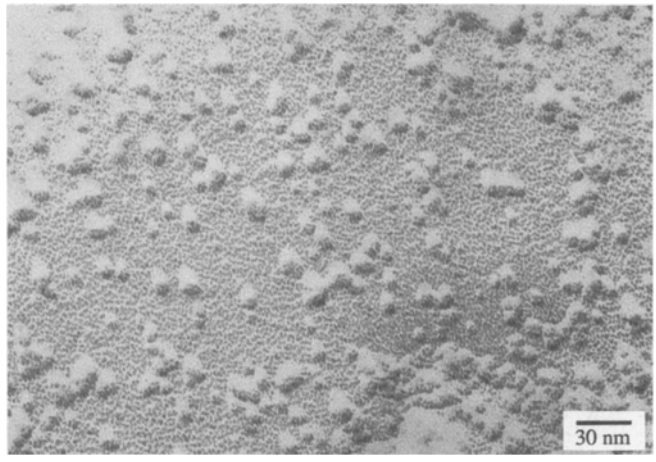

Fig. 4 Bright field image of platinum shadowed replica carried out by means of the freeze fracturing technique on overbased calcium salts (calcium excess of 100%). The micelles appear as small spherical particles, revealed by the platinum shadowing. Their mean diameter is of 100 ± 15 Å. The smooth aspect of the surface, between the particles, corresponds to the fracture through vitrified solvent

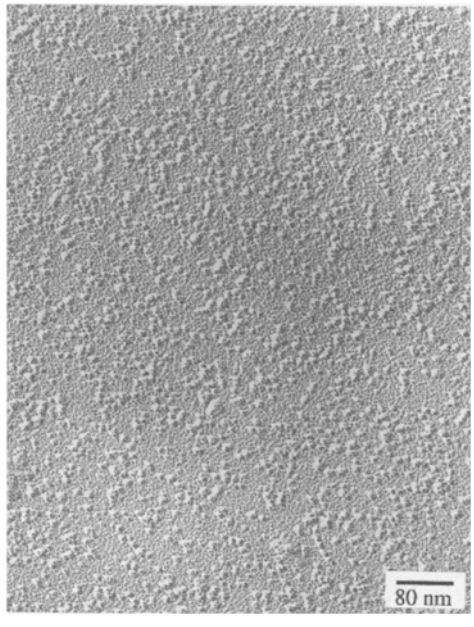

Fig. 5 Bright field image of platinum shadowed sample obtained by the direct deposit method on overbased calcium salts (calcium excess of 60%). The micelles appear as small spherical particles, revealed by the platinum shadowing. Their mean diameter is of 100 ± 15 Å

to the size of the platinum cluster ($\cong$ 15 Å) shadowing the sample. The absence of aggregate seems to show that in the case of the calcium salt, the direct deposit method does not introduce any artefacts of aggregation showing a high stability of the micellar structure as already noticed in the case of overbased calcium dodecyl benzene sulfonate micelles [11].

Figure 6 presents the micrograph and the electron diffraction pattern obtained on a nonshadowed part of the sample in order to investigate the structure of the mineral core. The diffraction pattern exhibits diffuse halos characteristic of an amorphous structure in agreement with previous EXAFS results [17]. The mineral core is clearly visible, but the phase contrast of the carbon support, in superposition, does not allows us to deduce a precise size of the mineral core.

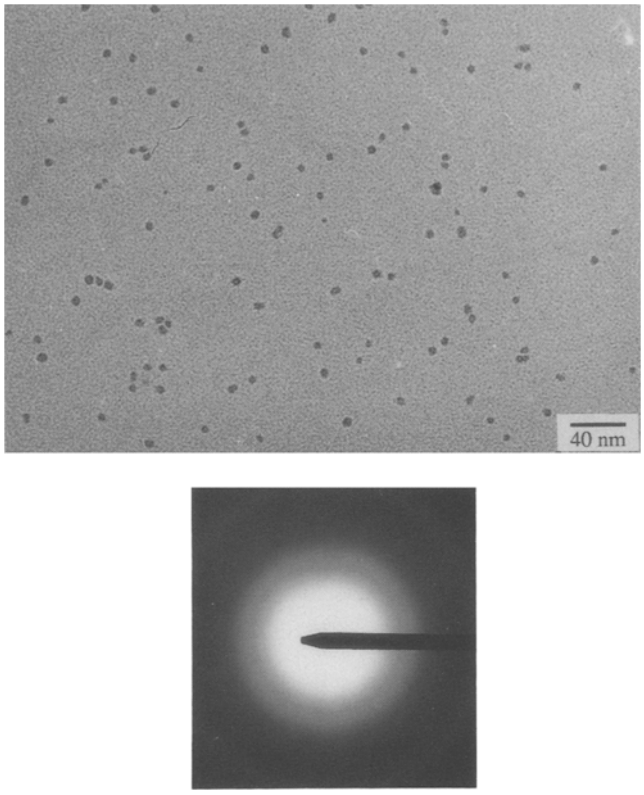

Fig. 6 Electron micrograph and diffraction pattern obtained on a non shadowed sample. The mineral calcium rich core of the micelles appears as small dark areas. The diffraction pattern only presents diffuse halos characteristic of a highly disordered structure

Quasi-elastic light scattering experiments

Two kinds of experiments were performed. First the samples were diluted with very pure grade heptane. In a second procedure the same samples were diluted with standard solvent (White spirit).

a) Samples diluted with pure heptane

The measurements were performed on dispersion in heptane of stoichiometric lead cekanoate (Figs. 7 and 8) and non-stoichiometric calcium cekanoate (calcium excess 60%, Figs. 9 and 10).

In these cases, the experiments do not present any major difficulties. Furthermore, the scattered intensity is very strong and the systems remain stable even at very low particle concentrations.

The results relative to calcium cekanoate dispersions reported in Figs. 9 and 10 shows the variations of $\langle\Gamma\rangle/2K^2$ and V with the volume fraction of the dispersed phase. One observes a leveling off of both $\langle\Gamma\rangle/2K^2$ and V for $\phi < 8\%$. This behaviour is typical of a dispersion of polydisperse hard spheres. In the dilute limit, the variations of

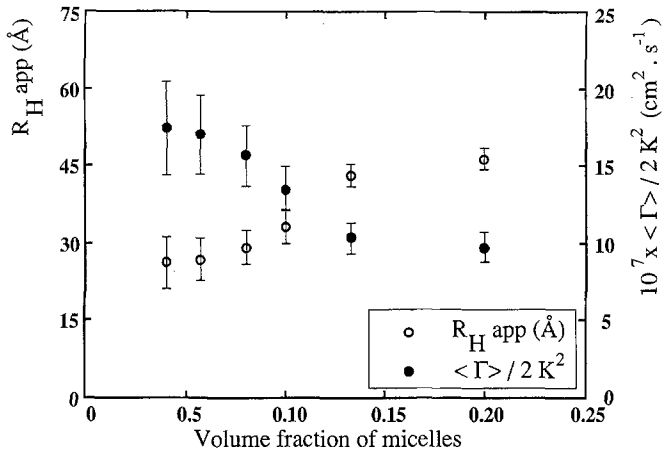

Fig. 7 Variations of $\langle\Gamma\rangle/2K^2$ and $\langle R_{Happ}\rangle$ with volume fraction of micelles for stoichiometric lead cekanoate. Solvent: heptane.

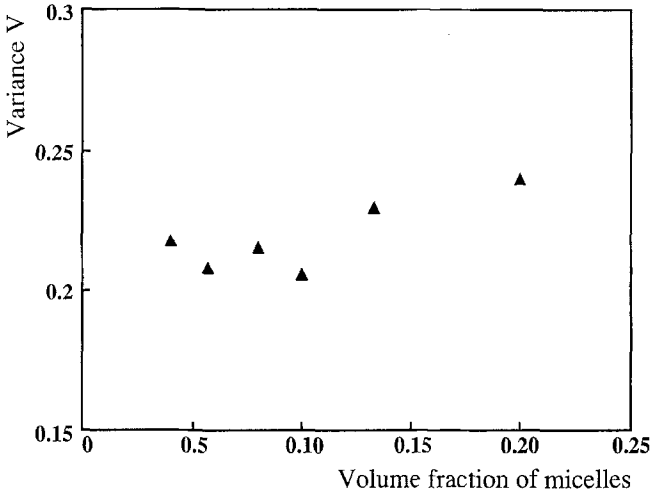

Fig. 8 Variations of the variance V of the autocorrelation function with volume fraction of micelles for stoichiometric lead cekanoate. Solvent: heptane

$\langle\Gamma\rangle/2K^2$ with ϕ obey Eq. (1) with a value of k_D slightly smaller than the theoretical value for hard spheres which suggests the existence of small attractive interactions.

From the extrapolation to zero volume fraction of $\langle\Gamma\rangle/2K^2$, one obtains the mutual diffusion coefficient:

$$D = [\langle\Gamma\rangle/2K^2]_{\varphi=0} = 19.6\ 10^{-7}\text{cm}^2.\text{S}^{-1}$$

Using the Stokes–Einstein equation

$$D = \frac{k_B T}{6\pi\eta R_H} \qquad (2)$$

One determines then the average hydrodynamic radius

$$\langle R_H\rangle = 29 \pm 3\ \text{Å}$$

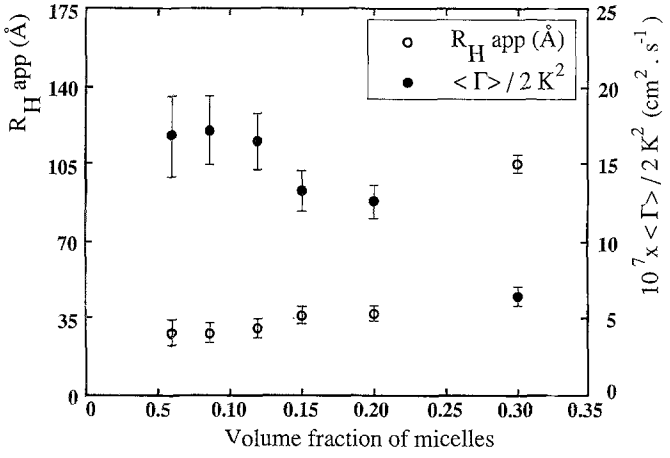

Fig. 9 Variations of $\langle\Gamma\rangle/2K^2$ and $\langle R_{Happ}\rangle$ with volume fraction of micelles for non stoichiometric calcium cekanoate (calcium excess 60%). Solvent: heptane

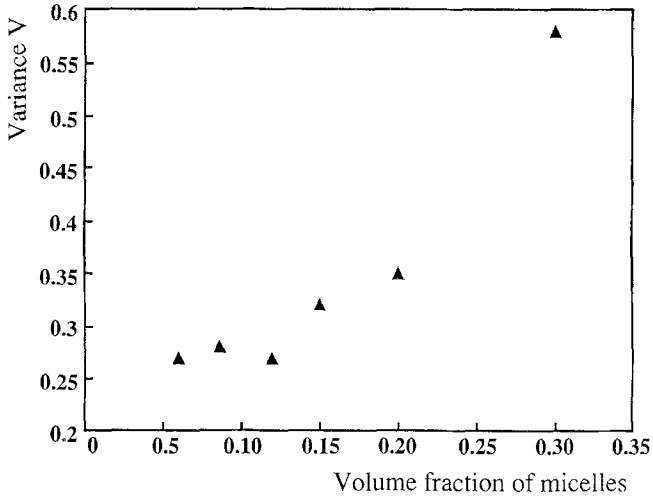

Fig. 10 Variations of the variance V of the autocorrelation function with volume fraction of micelles for the non stoichiometric calcium cekanoate (calcium excess 60%). Solvent: heptane

In the low volume fraction range, V is nearly constant and equal to 0.26, which is characteristic of a moderately broad size distribution. The decrease of $\langle\Gamma\rangle/2K^2$ in the high ϕ range, correlated with the increase of V, is likely to be due to the occurrence of slow modes associated with the self diffusion of particles [16]. In this study which is meant to characterize the structural properties of the dispersed particles, we have not tried to perform a bimodal analysis of the autocorrelation function which obviously would be more appropriate.

A similar behavior was observed for the dispersions of lead cekanoate. The evolution of $[\langle\Gamma\rangle/2K^2]$, $\langle R_H\rangle$ and V as a function of the micellar volume fraction are presented in Fig.s 7 and 8 and the extrapolated values of $\langle R_H\rangle$ at $\phi \rightarrow > 0$ are reported in Table 1, which summarizes the characteristics of the analyzed systems, together with the data obtained with transmission electron microscopy.

b) Samples diluted with standard solvent (white spirit).

Experiments on the systems diluted with standard solvent gave rise to several difficulties.

– The scattered intensity was very weak due to an insufficient refractive index contrast between the particles and the solvent.

– The scattered intensity was furthermore partially masked by an important fluorescence at the working wavelength of light (488 nm) which led us to the use of interferential filters.

Table 1 Micellar diameter (core + organic layer) obtained either through TEM or QELS

	white spirit dilution		heptane dilution				
	soi.lead cekanoate	non stoi clacium cekanoate	stoi. lead cekanoate			non stoi. calcium cekanoate	
	Q.E.L.S		Q.E.L.S	Cryo T.E.M.	direct deposit T.E.M	Q.E.L.S	Cryofract. T.E.M.
R_H	aggregates > 100 Å	aggregates > 100 Å	15 ± 5 Å	–	–	30 ± 5 Å	–
D_H	aggregates	aggregates	30 ± 10 Å	–	–	60 ± 10 Å	70 ± 15 Å
mineral core diameter	aggregates	aggregates	15 ± 5 Å	15 ± 5 Å	individual 15 ± 5 Å aggregates 60 ± 20 Å	45 ± 5 Å	55 ± 15 Å

– At strong dilution, a partial precipitation of the solute occurred. Furthermore, elastic light scattering experiments showed that under these conditions, at volume fraction, only a small amount of particles remained suspended in the solutions.

As the cekanoate dispersions are diluted with white spirit for industrial purposes, it was of interest to investigate the effect of the dilution by such a solvent on the structural properties of the particles.

Figure 11 shows the variations of $\langle\Gamma\rangle/2K^2$ and R_{Happ} with ϕ for a the lead cekanoate dispersion.

The apparent hydrodynamic radius R_{Happ} is defined by the same relation as (2) but at finite concentration.

One observes in the dilute regime a decrease of $\langle\Gamma\rangle/2K^2$ as the volume fraction is reduced, that can be associated with an increase of $\langle R_{Happ}\rangle$. As a matter of fact, at very low volume fraction, one can observe a partial precipitation of the lead cekanoate. Therefore, one can infer from these observations that dilution by white spirit tends to promote an irreversible aggregation of the particles. This is also confirmed by the increase of the variance with dilution (cf. Fig. 12). Similar behaviors were observed with the non-stoichiometric calcium cekanoate (Figs. 13 and 14). Such effects are likely due to the complex nature of the solvent, the latter being a mixture of alliphatic and aromatic compounds with very different solvation powers

Fig. 11 Variations of $\langle\Gamma\rangle/2K^2$ and $\langle R_{Happ}\rangle$ with volume fraction of micelles for the stoichiometric lead cekanoate. Solvent: white spirit

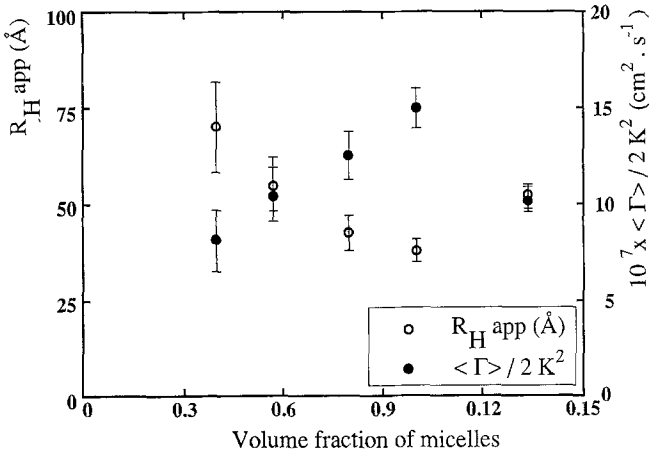

Fig. 12 Variations of the variance V of the autocorrelation function with volume fraction of micelles for the stoichiometric lead cekanoate. Solvent: white spirit

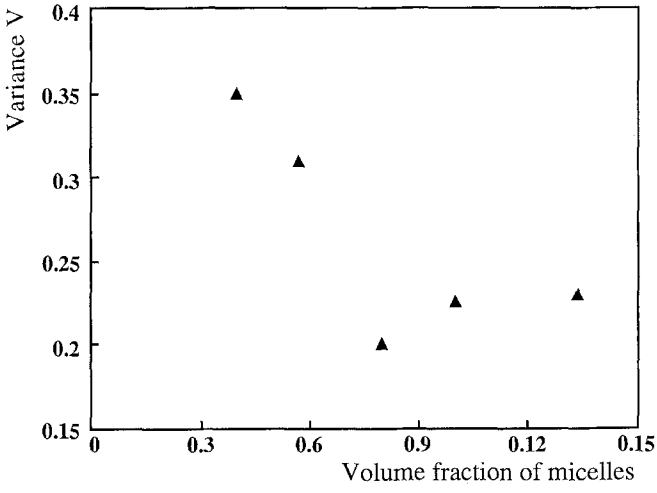

Fig. 13 Variations of $\langle\Gamma\rangle/2K^2$ and $\langle R_{Happ}\rangle$ with volume fraction of micelles for the non stoichiometric calcium cekanoate (calcium excess 60%). Solvent: white spirit

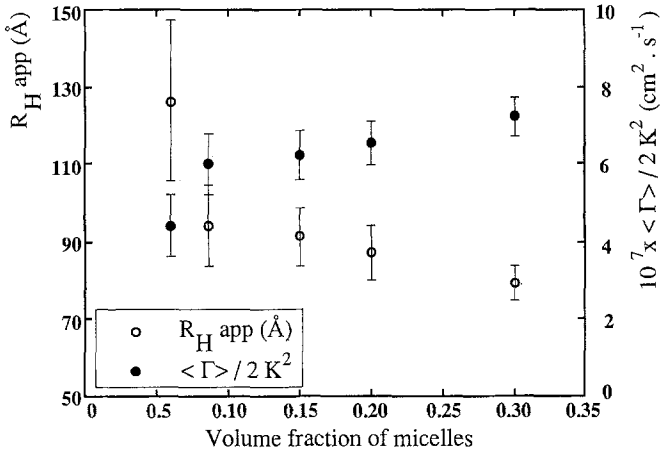

Fig. 14 Variations of the variance V of the autocorrelation function with volume fraction of micelles for the non stoichiometric calcium cekanoate (calcium excess 60%). Solvent: white spirit

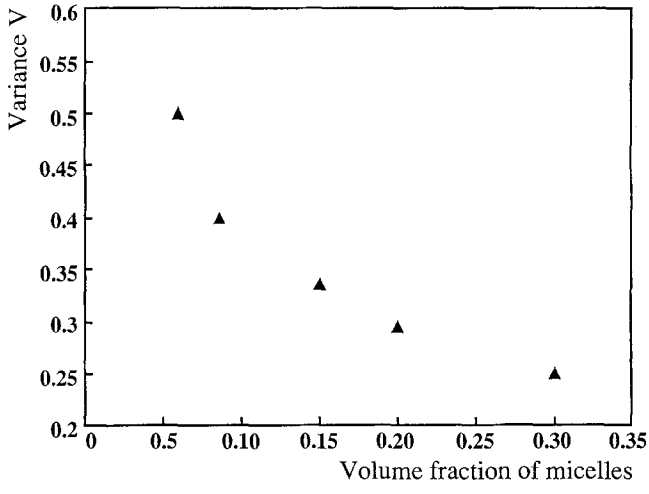

with respect to the metallic cekanoates. The cekanoate shells surrounding the metallic core of the dispersed particles might thus be preferentially solvated by some specific compounds of the solvent mixture, modifying the nature of the interactions and leading probably to precipitation.

Conclusion

Table 1 clearly shows that the two experimental approaches used in this work are able to provide complementary information. Particle diameters obtained by quasi-elastic light scattering are in agreement with those obtained by transmission electron microscopy. Furthermore the latter technique provides important information on the intimate structure of the mineral core. Finally, the results obtained in this study emphasize the influence of the environment of the micelles, especially the solvent used for dilution, on the stability of the dispersion.

References

1. Langevin D, Luisi P, Straub BE (ed) (1982) Reverse Micelles Plenum, New York, p 287
2. Marsh JF (1987) In Colloidal lubricant additives. Chemistry and Industry, pp 470–473
3. Mansot JL, Hallouis M, Martin J-M (1993) Colloids and Surfaces 75:25
4. Markovic I, Ottewill RH, Ottewill, Cebula DI, Field I, Marsh JF (1984) Colloid Polymer Sci, 262:648–656
5. Markovic I, Ottewill RH (1986) Colloid Polymer Sci, 264:67–76
6. Wéry J (1992) Thesis, University of Nantes
7. Belle C (1987) "Kinetics of calcium carbonate incorporation in micellar solution", Conference on microaggregates, Assise
8. Mansot J-L, Wéry J, Lagarde P, "Local structure analysis of the mineral core of reverse micelles in dispersion in hydrocarbons" (to appear)
9. Wéry J, Mansot J-L (1993) Microsc Microanal Microstruct, 4:87–100
10. Mansot J-L (1982) Thesis, ECLyon
11. Mansot J-L, Hallouis M, Martin J-M (1993) Colloids and Surface, 71:124
12. Candau S, Zana R (1981) J Coll Int Sci, 84:206
13. Koppel DE (1972) J Chem Phys, 57:4814
14. Brown JC, Pusey PN, Dietz R (1975) J Chem Phys, 62:1136
15. Pusey PN, Fijnaut HM, Vrij A (1982) J Chem Phys, 77:4270
16. Pusey PN (1984) J Chem Phys, 80:8
17. Mansot et al., J-L (1989) Physica B, 158:237